Novel Application Method for Mesenchymal Stem Cell Therapy Utilizing Its Attractant-Responsive Accumulation Property

上田, 将之

https://doi.org/10.15017/4060079

出版情報：九州大学, 2019, 博士（歯学）, 課程博士
バージョン：

applied sciences

MDPI

Article

Novel Application Method for Mesenchymal Stem Cell Therapy Utilizing Its Attractant-Responsive Accumulation Property

Nobuyuki Ueda [1], Ikiru Atsuta [2,*], Yasunori Ayukawa [1], Takayoshi Yamaza [3], Akihiro Furuhashi [1], Ikue Narimatsu [1], Yuri Matsuura [1], Ryosuke Kondo [1], Yu Watanabe [1], Xiaoxu Zhang [1] and Kiyoshi Koyano [1]

1 Section of Implant and Rehabilitative Dentistry, Division of Oral Rehabilitation, Faculty of Dental Science, Kyushu University, Fukuoka 812-8582, Japan; nobuyuki@dent.kyushu-u.ac.jp (N.U.); ayukawa@dent.kyushu-u.ac.jp (Y.A.); furuhasi@dent.kyushu-u.ac.jp (A.F.); narimatu.i@dent.kyushu-u.ac.jp (I.N.); lily1225@dent.kyushu-u.ac.jp (Y.M.); r.kondo@dent.kyushu-u.ac.jp (R.K.); yu-w-23@dent.kyushu-u.ac.jp (Y.W.); xiaoxu3535@dent.kyushu-u.ac.jp (X.Z.); koyano@dent.kyushu-u.ac.jp (K.K.)

2 Division of Advanced Dental Devices and Therapeutics, Faculty of Dental Science, Kyushu University, Fukuoka 812-8582, Japan

3 Division of Oral Biological Sciences, Department of Molecular Cell Biology and Oral Anatomy, Kyushu University, Fukuoka 812-8582, Japan; yamazata@dent.kyushu-u.ac.jp

* Correspondence: atyuta@dent.kyushu-u.ac.jp; Tel.: +81-92-642-6441

Received: 12 September 2019; Accepted: 2 November 2019; Published: 15 November 2019

Featured Application: We developed a remote administration method of Mesenchymal Stem Cells with therapeutic characteristic that used collagen gel as a scaffold.

Abstract: Stem cell therapy is an emerging treatment modality for various diseases. Because mesenchymal stem cells (MSCs) are known to accumulate at the site of damage, their possible clinical application has been investigated. MSCs are usually administered using intravenous injection, but this route carries a risk of pulmonary embolism. In contrast, topical injection of MSCs reportedly has an inferior therapeutic effect. We developed a remote administration method that uses collagen gel as a scaffold and investigated the effect of this scaffold on the retention of stemness, homing ability, and therapeutic effect using a mouse tooth extraction model. After verifying the retention of stemness of MSCs isolated from the bone marrow of donor mice in the scaffold, we administered MSCs subcutaneously into the back of the recipient mice with scaffold and observed the accumulation and the acceleration of healing of the extraction socket of the maxillary first molar. The MSCs cultured with scaffold retained stemness, the MSCs injected into back skin with scaffold successfully accumulated around the extraction socket, and socket healing was significantly enhanced. In conclusion, administration of MSCs with collagen scaffold at a remote site enhanced the lesion healing without the drawbacks of currently used administration methods.

Keywords: mesenchymal stem cell; tooth extraction socket; collagen gel; systemic administration; wound healing; scaffold

1. Introduction

Mesenchymal stem cells (MSCs), which are known to contribute to tissue regeneration and repair [1] are normally present in a dormant state in almost all organs [2]. Upon the release of cytokines by a stimulus such as inflammation or tissue injury, MSCs begin to proliferate and migrate

to where cytokines are being released [3]. However, proliferation and migration of MSCs take time, and a lack of MSCs at required sites may impede tissue healing. Although some methods utilize the regenerative properties of stem cells for therapy [4], in terms of cell delivery methods, a gold standard has not been established and further study is needed. For current cell therapies, MSC administration routes include intra-arterial/intravenous, intraperitoneal, and direct administration into tissues and organs. These methods can roughly be classified into two groups: systemic administration and local administration. Systemic administration is a well-documented method [5,6] whereby MSCs are applied in the cardiovascular system and reach the damaged area through circulating blood. However, fewer than 10% of administered MSCs accumulate at the site of damage, with many cells becoming captured in the lungs [7–10].

Local administration of MSCs to the injury site has advantages, such as a rapid and localized reaction [11]. However, it involves risks such as cells inducing apoptosis when administered at high density [12], or bleeding and secondary damage caused by the administration itself. For these reasons, treatment outcomes are not always stable and the ideal administration method has not yet been established for MSC-based therapies.

Therefore, we focused on the potential of MSCs to autonomously accumulate in damaged tissue [13–15]. Our hypothesis is that subcutaneous administration of a mixture of scaffold and MSCs into the body, such as under the easily accessible back skin, will result in MSCs autonomously migrating from the scaffold to the site where cytokines are produced and enhancing tissue repair [16]. Collagen gel, which has high biocompatibility and is easily applied in the clinic, was used as a scaffold to administer a sufficient number of stem cells in this study. We investigated the migration of delivered stem cells and the healing of a tooth extraction site, where both soft and hard tissue healing are involved.

2. Materials and Methods

2.1. Animals

Male C57BL/6N mice (6 weeks of age; Kyudo Laboratories, Tosu, Japan) and male green fluorescent protein (GFP)-transgenic C57BL/6N mice (CAG-EGFP; 6 weeks of age; Japan SLC, Shizuoka, Japan) were used in this study. All animal experiments were performed under an institutionally approved protocol for the use of animals in research at Kyushu University (approval number: A29-237-0), (approval day: 29 July 2016).

2.2. Isolation and Culture of MSCs

MSCs were isolated from the bone marrow of mice as described previously [17]. Briefly, bone marrow cells were flushed out from the femoral and tibial bone cavities of the mice. The cells were passed through a 40-μm cell strainer to obtain a single-cell suspension, which was seeded in 100-mm culture dishes at 1×10^6 cells/dish. One day after seeding, cells were washed with phosphate-buffered saline (PBS) and cultured in growth medium comprising alpha-minimum essential medium (α-MEM; Invitrogen, Grand Island, NY, USA) supplemented with 20% fetal bovine serum (FBS; Equitech-Bio, Kerrville, TX, USA), 2 mM L-glutamine (Invitrogen), 100 U/mL penicillin (Invitrogen), and 100 μg/mL streptomycin (Invitrogen).

2.3. Osteogenic Differentiation Assay

To confirm calcium deposition, MSCs were seeded on 35-mm dishes at 2.5×10^5 cells/dish, grown to confluence in growth medium, and then cultured in osteogenic culture medium (growth medium containing 1.8 mM KH_2PO_4 and 10 nM dexamethasone; both from Sigma-Aldrich, St. Louis, MO, USA). After 28 days of osteogenic induction, cultures were stained with 1% alizarin red S solution (Sigma-Aldrich). Measurement of the positive area of alizarin red was performed using Image J (National Institutes of Health, Bethesda, MD, USA) [18].

2.4. Adipogenic Differentiation Assay

MSCs were seeded on 35-mm dishes at 2.5×10^5 cells/dish, grown to confluence in growth medium, and then cultured in adipogenic culture medium (growth medium containing 0.5 mM isobutylmethylxanthine, 60 µM indomethacin, 0.5 µM hydrocortisone, and 10 µg/mL insulin; all from Sigma-Aldrich). After 14 days of adipogenic induction, cultures were stained with oil red O. The oil red O-positive lipid droplets were observed using an inverted microscope (BZ-9000; Keyence, Osaka, Japan).

2.5. CFU-F Assay

The CFU-F assay was performed as described previously [17]. Passage 1 MSCs were seeded into culture dishes (Nalge Nunc, Rochester, NY, USA). After 16 days of culture, cells were stained with a solution of 0.1% toluidine blue and 2% paraformaldehyde. Total colony numbers were counted per dish. Three independent experiments were performed. Measurement of the positive area of toluidine blue was performed using Image J [18].

2.6. MSC Injection Via the Tail Vein

GFP-MSCs isolated from the bone marrow of transgenic mice were cultured and passaged three times before injection. Mice (n = 5 per group) were anesthetized by combined anesthesia (0.3 mg/kg medetomidine, 4.0 mg/kg midazolam, 5.0 mg/kg butorphanol) and ex vivo-expanded MSCs (1×10^6 cells in 2 mL of PBS) were administered via the tail vein at 48 h before tooth extraction. Control mice (n = 5) were injected with PBS via the tail vein.

2.7. MSC Injection into the Back of Mice

GFP-MSCs and mice were prepared as above. The ex vivo-expanded MSCs (1×10^6 cells in 2 mL of PBS) were then administered into the back of the mice subcutaneously at 48 h before tooth extraction. Control mice (n = 5) were injected with PBS via the same route.

2.8. Cell Cultures

For in vitro assessment, MSCs were seeded on 35-mm dishes at 2×10^4 cells/dish and incubated for 12 h at 37 °C under 5% CO_2. A subset of MSCs was incubated in medium containing 100 nM chloromethyltetramethylrhodamine (MitoTracker Orange CMTMRos; Molecular Probes, Eugene, OR, USA) for 20 min at 37 °C in the dark. After three washes with medium, these cells were examined under an inverted fluorescence microscope (BZ-9000).

2.9. Collagen Gel Culture

MSCs were embedded three-dimensionally in the collagen gel. Neutralized collagen solution was prepared by mixing eight volumes of Cellmatrix type I-A (Nitta Gelatin, Osaka, Japan) with one volume of 10× α-MEM and reconstitution buffer (2.2 g $NaHCO_3$ in 100 mL of 0.05 N NaOH and 200 mM HEPES). The solution contained type I collagen at a final concentration of 2.4 mg/mL. To prevent cell attachment and growth directly on cell culture dishes, 1 mL of plain collagen solution was poured into each culture dish as a base layer. MSCs were suspended in neutralized collagen mixture at a density of 1.0×10^6 cells/mL of gel. After allowing the base layer to solidify with a short incubation at 37 °C, 1 mL of neutralized collagen mixture containing cells was added. After the top gel layer was formed by additional incubation at 37 °C for 15 min, 1.5 mL of culture medium (α-MEM with 2.5% FBS and antibiotics) was added into the culture dish. The medium was changed every 3 days [19,20].

2.10. Counting of MSCs in Collagen

To isolate the MSCs from 3D culture with collagen gel, the collagen gel was dipped into a digestion solution with 10× α-MEM, dispase II (Godo Shusei, Tokyo, Japan), collagenase L (Nitta Gelatin),

and $NaHCO_3$ (Nacalai Tesque, Kyoto, Japan) for 30 min at 37 °C. The MSCs were then collected by centrifuging using a table top centrifuge (Kubota, Tokyo, Japan) at 367× *g* for 5 min, and counted using an automated cell counter (TC20; Bio-Rad Laboratories, Hercules, CA, USA).

2.11. The Injection of Collagen Gel with MSC

To prepare a homogeneous mixture, MSCs (1.0×10^6 cells) were stirred on ice with a mixed solution of 1.6 mL of collagen gel (Cellmatrix type IA) and 0.4 mL of reconstitution buffer. Next, mice (n = 5 per group) were anesthetized using a combination anesthetic (described above), and 2 mL of collagen gel containing MSCs was injected into the back of each mouse subcutaneously using a 5-mL syringe (Terumo, Tokyo, Japan) and 25-G injection needle (Terumo). MSCs were administered at the intersection between the straight line connecting the median line and the shoulder blades on both sides of the mice.

2.12. Counting of Injected MSCs in Collagen Gel

Mice were deeply anesthetized and the scaffold was removed from the back of the mice. The collected scaffold was fixed in 4% paraformaldehyde (pH 7.4). Frozen samples were cut into 10 µm-thick sections with a cryostat at −20 °C. After choosing 10 sections from every 10 slices, they were stained and examined under an inverted fluorescence microscope (BZ-9000) by counting cells in a visual field region (500 × 500 µm) in random areas. Then, the average number of cells was determined.

2.13. Counting of Injected MSCs at Tooth Extraction Site and Organs

Mouse maxillary first molars were extracted under a combination anesthetic. Three days after tooth extraction, mice were deeply anesthetized and perfused intracardially with heparinized PBS. As controls, mice were subjected to tooth extraction but not administered MSCs. Intact maxilla, kidney, liver, lung, spleen, femur, and tibia were harvested en bloc. After preparing frozen sections, 10 sections were selected from every 10 slices to observe GFP-MSCs that accumulated in each organ. The sections were stained, and the number of cells were counted.

2.14. Tissue Preparation

For in vivo assessment, tissues were prepared according to our previously described methods [21,22]. At the end of each experimental period, mice were euthanized under combination anesthesia and perfused intracardially with heparinized PBS, followed by 4% paraformaldehyde (pH 7.4). Maxillae were demineralized in 5% EDTA for 4 days at 4 °C. Prepared sites were cut into 10-µm buccopalatal sections with a cryostat at −20 °C.

2.15. Immunofluorescence Microscopy

Immunofluorescence staining of in vitro and in vivo samples was carried out by blocking samples with normal serum (matched to the secondary antibody) for 1 h, followed by incubation with mouse anti-rat GFP, CD29, CD45, CD90, and CD105 antibodies (1:100; Sigma-Aldrich) overnight at 4 °C. Samples were then treated with a fluorescein isothiocyanate-conjugated secondary antibody (1:200; Jackson ImmunoResearch, West Grove, PA, USA) for 1 h at room temperature (RT) and mounted with 4′,6-diamidino-2-phenylindole (DAPI). A subset of sections was stained with Azan stain [23].

2.16. Expression of Adhesion Protein

To observe the primary epithelial closure of the tooth extraction cavity, laminin (Ln)-332 was immunostained to confirm the continuity of the epithelium (the distance between edges of basement membranes). Tissue sections were blocked with 10% normal goat serum (Vector Laboratories, Burlingame, CA, USA) for 30 min at RT. Sections were stained using rabbit anti-mouse Ln-332 (1:100, Santa Cruz Biotechnology, Santa Cruz, CA, USA) antibodies (1:100, Sigma-Aldrich) diluted

in antibody dilution solution for 18 h at 4 °C. Finally, samples were treated with fluorescein isothiocyanate-conjugated secondary antibody (1:200; Jackson ImmunoResearch) for 1 h at RT [21].

2.17. Statistical Analysis

Data are expressed as mean ± standard deviation (SD). Student one-way analysis of variance with Tukey's range test or *t*-test was performed. Values of $p < 0.05$ were considered significant. Experiments were performed using triplicate samples and repeated three or more times to verify their reproducibility.

3. Results

3.1. MSC Behavior in Collagen Gel Scaffold (In Vitro Study)

Figure 1A shows the experimental schedule and method used in the study. The number of MSCs remaining in the scaffold at 21 days was significantly decreased compared with the number on other days (Figure 1B). During the first 14 days, MSCs retained their original characteristics, including abilities for self-renewal and multi-directional differentiation. As shown in Figure 1C, MSCs maintained expression of MSC positive markers (CD29, CD90, and CD105) without expressing negative marker (CD 45) could differentiate into adipocytes or osteoblasts based on oil red O or alizarin red S staining, respectively, and formed colonies from single cells.

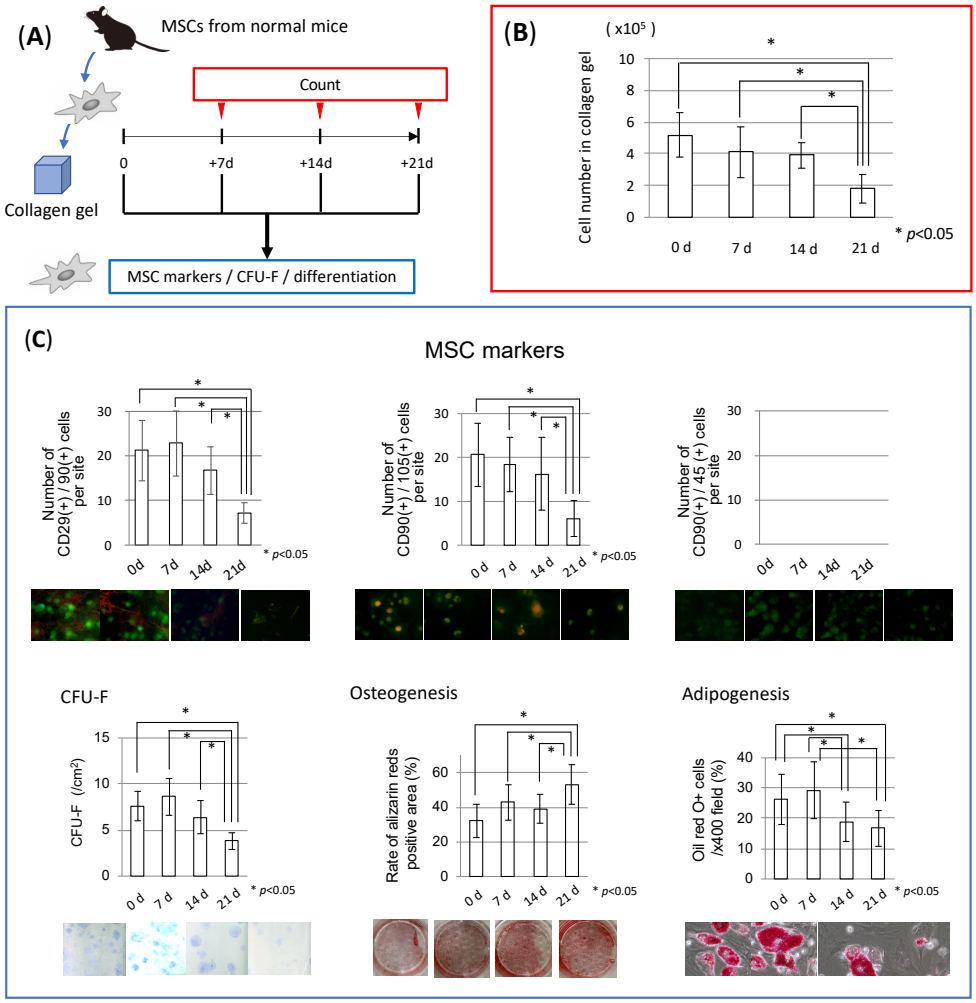

Figure 1. Mesenchymal stem cells (MSCs) state in collagen gel. (**A**) Experimental protocol for the in vitro study. MSCs isolated from wild-type C57BL/6N mice were cultured in a collagen gel for 3 weeks.

(**B**) Numbers of surviving MSCs in the scaffold. After the 3-week culture in collagen gel, numbers of cells were evaluated. MSCs could remain alive for at least 14 days. (**C**) Retention of MSC characteristics. After the 3-week culture in collagen gel, isolated cells were checked for the characteristics of MSCs, including self-renewal, multi-directional differentiation, and expression of MSC original markers (CD29, CD90, and CD105). (Top left) There were many CD29/CD90 double-positive cells for 14 days. (Top middle) There were many CD90/CD105 double-positive cells for 14 days. (Top right) There were no CD90/CD45 double-positive cells. (Bottom left) CFU-F of MSCs. MSCs cultured for 21 days generated fewer CFU-Fs compared with MSCs at other time points. (Bottom middle) Osteogenic differentiation of MSCs. MSCs cultured under osteogenic differentiation conditions for 4 weeks were stained with alizarin red S. (Bottom right) Adipogenic differentiation of MSCs. MSCs cultured under adipogenic differentiation conditions for 3 weeks were stained with oil red O. All data indicated that stemness may be retained for up to 14 days. * $p < 0.05$.

3.2. Stability of Collagen Gel in the Body (In Vivo Study)

Figure 2A shows the experimental schedule and method used in the study. MSCs were injected with collagen gel into the subcutaneous tissue of mice. The appearances of mice backs immediately, 7 days, and 14 days after collagen injection are shown in Figure 2B. Until 7 days after collagen injection, the collagen retained its shape without significant changes. Additionally, as shown in Figure 2C, the gel showed some changes in the number of GFP/CD90-positive cells over 2 weeks. Thus, MSCs decreased gradually from the scaffold after 2 weeks in vivo.

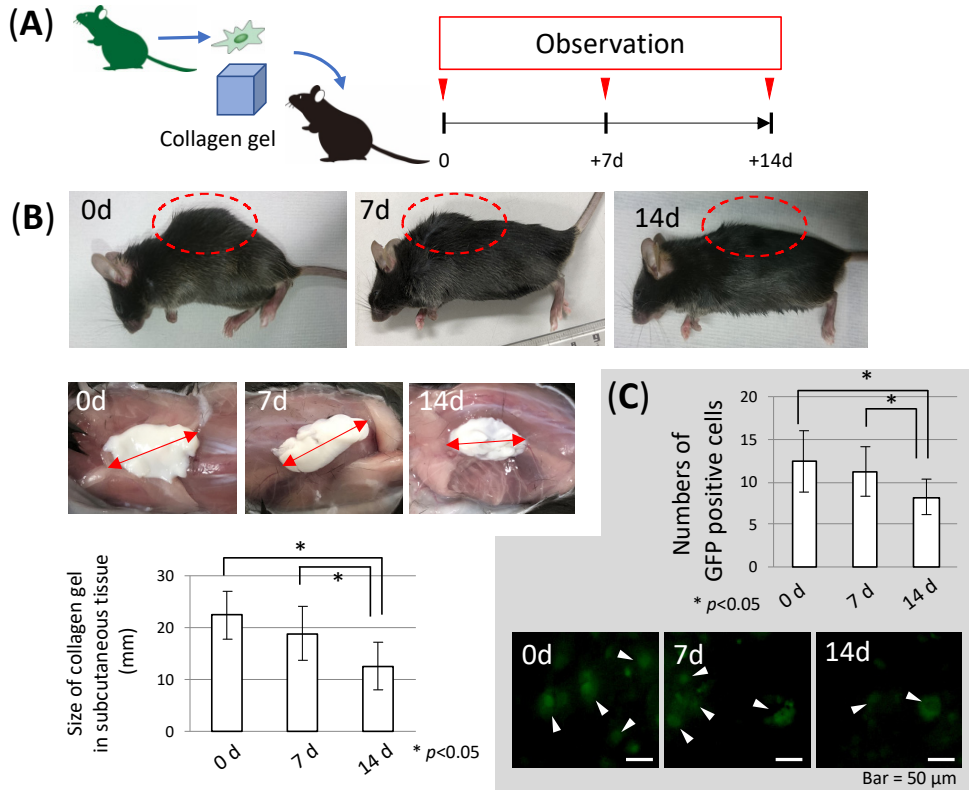

Figure 2. MSC stability in a subcutaneously implanted collagen scaffold. (**A**) Experimental protocol for in vivo experiments. (**B**) (Upper) Appearances of mice backs after collagen injection (immediately, 7 days, and 14 days after injection). (Lower) Shapes of collagen gels in the backs of mice (immediately, 7 days, and 14 days after injection). The size of the collagen gel decreased over time. (**C**) Numbers of green fluorescent protein (GFP) positive cells in collagen gels at time of injection and upon removal from mice backs at 2 weeks after injection (Number of cells per 500 × 500 μm field in section). More than half the cells remained alive for 2 weeks. * $p < 0.05$.

3.3. Changes in Cell Number in Scaffolds before and after Tooth Extraction

Figure 3A shows the experimental schedule and method used in the study. After tooth extraction, the number of MSCs in the scaffold decreased significantly compared with the number before extraction (Figure 3B). In particular, at 5 and 7 days after collagen injection with MSCs, there was a large difference between extraction and non-extraction groups.

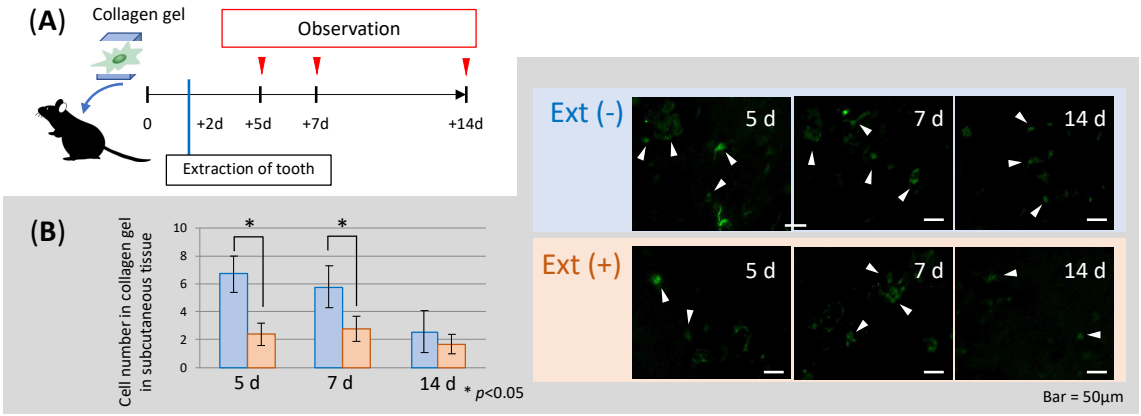

Figure 3. Changes in cell number in the scaffold after tooth extraction. (**A**) Wild-type C57BL/6N mice received tooth extraction 2 days after collagen injection with MSCs. After further 3, 5, or 12 days, the numbers of cells in the collagen gel were compared between extraction and no-extraction groups. (**B**) In the extraction group (5 and 7 days), a remarkable reduction of cells in the scaffold was observed (Number of cells per 500 × 500 μm field in section). * $p < 0.05$.

3.4. Accumulation of MSCs in Several Organs

Figure 4A shows the experimental schedule and method used in the study. Numbers of accumulated MSCs in lung, kidney, liver, spleen, and bone marrow after MSC injection via the tail vein and injection of collagen gel with MSC are shown in Figure 4B. In particular, the lung accumulated a large number of MSCs in MSC injection via the tail vein. MSCs were not observed except in the lungs of the collagen group. As shown in Figure 4C, mice injected with MSCs in the scaffold or via the back accumulated much lower numbers of MSCs in the lung than those injected with MSCs via the tail vein.

3.5. Effect of Delivering MSCs with a Scaffold on Epithelial Healing after Tooth Extraction

Figure 5A shows the experimental schedule and method used in the study. In mice injected with MSC via the tail vein and in the scaffold MSC groups, many GFP/CD90 double-positive cells were observed around the socket after tooth extraction (Figure 5B). The numbers of MSCs were similar in the scaffold MSC and tail vein-injected MSC groups. Although both control groups exhibited poor healing, the scaffold MSC group showed good mucosal healing, similar to the injected MSC group (Figure 5C). Immunohistochemical staining with Ln-332 revealed the degree of epithelial healing (Figure 5D). The data indicated that scaffold MSC had epithelial continuity similar to that of tail vein-injected MSC.

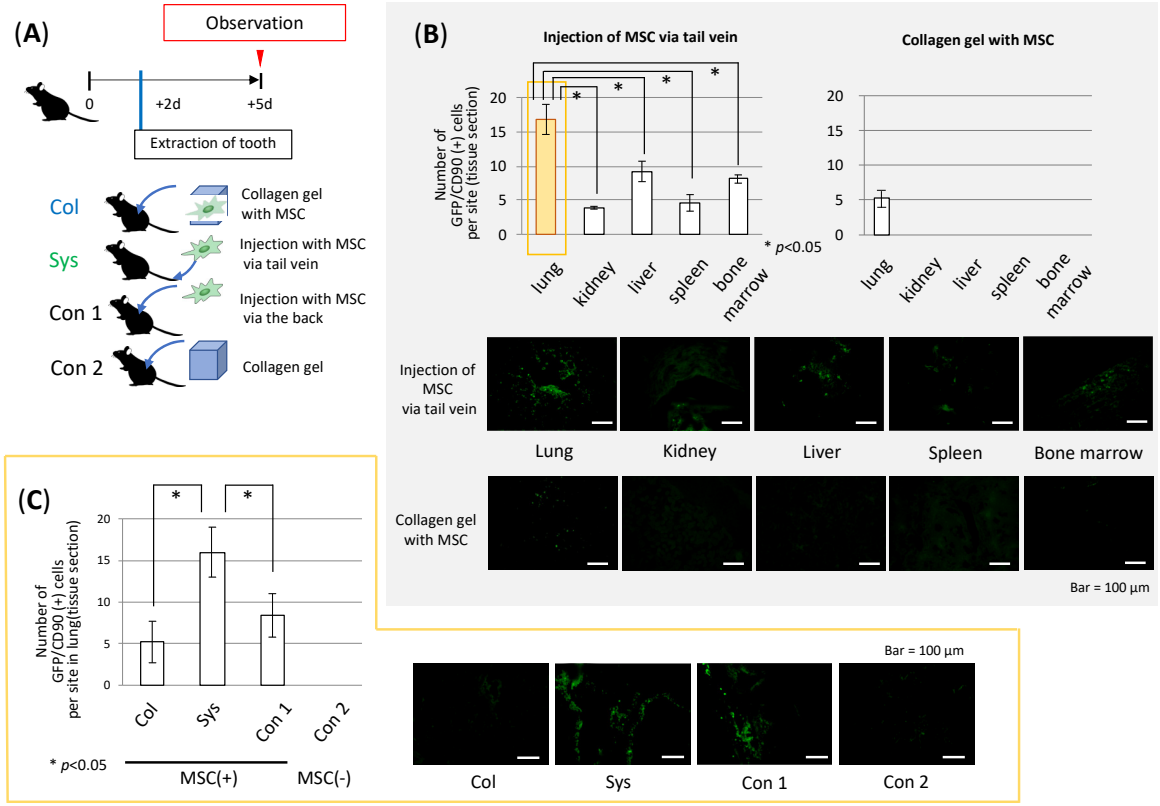

Figure 4. Accumulation of MSCs into organs following tooth extraction. (**A**) Experimental protocol for in vivo experiments. (**B**) Numbers of MSCs in several organs. At 5 days after systemic injection via the tail vein and injection of collagen gel with MSC, cell numbers in the lung, kidney, liver spleen, and bone marrow were counted and plotted. In particular, the lung accumulated a large number of MSCs. Scale bar, 100 μm. (**C**) As novel and conventional methods, MSCs isolated from GFP-transgenic mice were cultured with or without a collagen gel and injected into mice 2 days before tooth extraction. At 5 days after MSC administration, the number of cells accumulated in the lung was evaluated. Systemic injection via the tail vein resulted in significantly higher numbers of MSCs in the lung than in the collagen group or in mice injected in the back with MSCs. Scale bar, 100 μm. * $p < 0.05$.

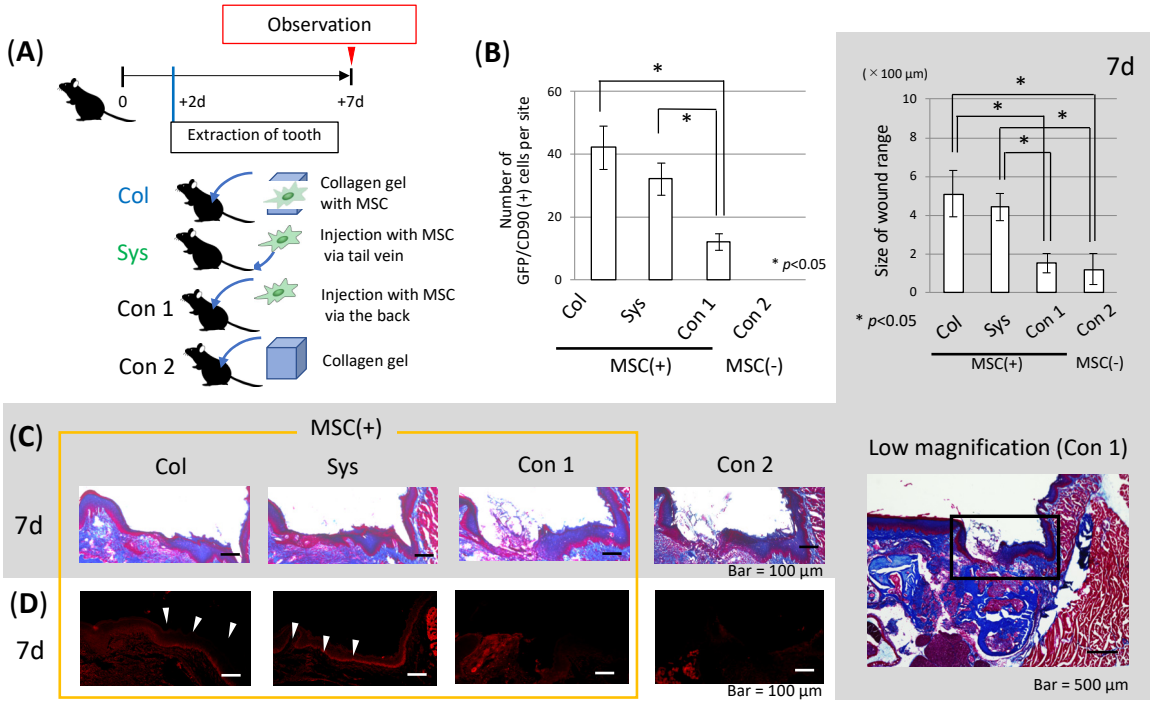

Figure 5. Effect of MSCs from collagen gel for tooth extraction. (**A**) Experimental protocol for in vivo experiments. (**B**) At 7 days after MSC administration, numbers of accumulated MSCs around the tooth extraction socket. MSCs injected via the tail vein and MSCs from collagen gel were observed as many GFP/CD90 double-positive cells around the socket after extraction by immunofluorescence staining. Injected MSCs accumulated similarly to scaffold MSCs. (**C**) Extraction socket healing. The scaffold MSC group and the injected MSC group showed good mucosal healing at 7 days. Scale bars, 100 μm. * $p < 0.05$. (**D**) localization of Ln-332. Laminin-332 was observed as a line on connective tissue in both the systemic injection and collagen scaffold groups (white arrowheads).

4. Discussion

Recently, clinical research of stem cell therapies has been increasing. Although the mechanisms underlying the therapeutic benefit of stem cells remain unclear, many reports suggest the efficacy of related cell therapies [24,25]. In this study, two mechanisms of enhanced healing of the tooth extraction site can be assumed. First, administered MSCs differentiate into gingiva cells and facilitate wound closure. Second, MSCs secrete cytokines and growth factors that activate epithelial cells to migrate and proliferate to achieve primary closure of the damaged tissue [26].

We previously reported that intravenous administration of MSCs in rats contributed to the healing of damaged tissue [27]. However, delivering cells subcutaneously without a scaffold did not result in a positive effect on tissue healing [28]. As such, we focused on the scaffold as a foundation for cells.

First, we searched for a suitable scaffold material in which MSCs could retain their characteristics for long periods of time. Although we verified the competence of other materials (data not shown), we selected collagen as a scaffold because it is fluid at low temperatures, which makes it easy to deliver by injection and less damaging to the cells. In addition, collagen forms a gel at body temperature, which facilitates retention at the application site [29]. Generally, if artificial materials exist in the body for a long time, problems such as infection or degradation may arise; thus, the characteristics of type I collagen, which can be absorbed by the body, might be suitable. In addition, collagen seems to provide an effective scaffold with little toxicity, as suggested by other studies [30,31].

Consistent with previous reports [32,33], MSCs could remain alive in the scaffold without major changes in cell number for 2 weeks. Meanwhile, as shown in Figure 1C, MSCs maintained expression of MSC markers (CD29, CD90, and CD105), and MSCs extracted at each stage exhibited differentiation

and self-renewal potential. Therefore, MSCs could maintain their "stemness", which is an important characteristic for at least 14 days.

Second, we checked the competence of collagen as a scaffold. As shown in Figure 2A, the injected 2 mL of collagen retained its form at 2 weeks after insertion into back subcutaneous tissue. Our results were consistent with previous reports suggesting that a 2-week period was required to absorb approximately 5-mm diameter (corresponding to 2 mL) of collagen containing MSCs after insertion into the body as a scaffold for exogenous cells [34]. Safety of the collagen scaffold was determined by the survival rate of MSCs in the scaffold in vivo experiments. As a result, MSCs in collagen gels implanted in back subcutaneous tissue remained alive for at least 2 weeks, similar to the in vitro data shown. Thus, the injected collagen scaffold had the potential to act as a reservoir for exogenous MSCs in the body.

Third, we investigated whether MSCs in the collagen gel could maintain their chemotactic properties. A previous report indicated that systemically delivered MSCs accumulated at sites of inflammation [27,35]. As shown in Figure 3, MSCs could be guided from the collagen scaffold to the wound area after tooth extraction. However, most MSCs remained in the scaffold when tooth extraction was not performed. MSCs in the collagen gel seemed to have the ability to accumulate at a wound site via the systemic circulation. Therefore, we examined the localization of the MSCs after they migrated from the collagen scaffold, as shown in Figure 4.

Regarding the effect of administration method, we previously conducted a study comparing systemic and topical administration, which suggested that subcutaneous administration of MSCs was ineffective when not applied with a scaffold [28]. Similar to previous findings [36,37], the lung and liver accumulated many cells from the systemic circulation. In this experiment, many MSCs were observed in the lung following systemic administration without using scaffolds, but there was only a slight accumulation in the lung when the MSCs were injected within a collagen scaffold. After tooth extraction, fewer MSCs from the collagen scaffold were observed in the lung but could be seen in the wound area. Therefore, delivering MSCs within a scaffold may decrease the risk of lung or cardiac infarction. As MSCs are adherent cells, they readily form cell aggregates immediately after isolation from culture dishes [38]. Thus, when injected via the tail vein, most of the cells formed a mass. This might explain why intravascularly applied cells have higher risks for capture in capillary-like lung tissue. In contrast, cells migrating from the scaffold should move individually, making them less likely get clogged in the lung, which is supported by our results.

Finally, we investigated the effect of MSCs with a collagen scaffold. As mentioned before, many reports suggest that MSCs could accumulate in the wound area after systemic administration [39]. As shown in Figure 5B, many cells were observed around the extraction site following conventional systemic injection, but a similar number of cells were observed around the site in the scaffold group. Both groups showed similar promotion of wound healing after tooth extraction, compared with both control groups (Figure 5C). On the contrary, we recently reported that the high density of MSCs at the injected site following local administration meant that it was hard for them to move from the administration site to the site of inflammation [28].

In the scaffold group, the cells present in a suitable space in the collagen apparently maintained their MSC properties. This indicates that side effects such as pulmonary embolism may be avoided by using collagen scaffolds, and that this process may also contribute to tissue healing.

The amount of cytokines released from the wound site is reported to closely correlate with the degree of inflammation [40]. In addition, MSC migration in response to cytokines has been shown to occur in a dose-dependent manner [41]. This suggests that when severe damage occurs in a tissue, increased inflammation and cytokine release elicit migration of MSCs to that area. Based on this concept, our delivery method should control the number of MSCs migrating to the damaged site depending on the degree of damage, which may overcome some of the disadvantages of existing cell delivery methods.

5. Conclusions

In summary, administering stem cells remotely via a collagen scaffold and allowing cells to migrate autonomously to the damaged area is advantageous for delivery of cell therapies. This novel method has great potential for both the treatment and prevention of tissue damage, given the ability of MSCs to detect abnormal and damaged cells. MSC-based therapy using a collagen scaffold may thus offer a safer and more effective therapeutic modality for various systemic diseases.

Author Contributions: N.U., I.A., Y.A., I.N., and Y.M. were involved in the practical aspects of experiments. N.U., I.A., Y.A., T.Y., R.K., Y.W., and X.Z. collected, analyzed, and interpreted the data. I.A. designed the study and provided financial and administrative support. I.A., Y.A., T.Y., A.F., and K.K. wrote the manuscript. I.A., T.Y., A.F., and K.K. revised the manuscript for publication. Each author participated sufficiently in the work to take public responsibility for appropriate portions of the content.

Funding: This research was funded by JSPS KAKENHI [Grant Number JP17K17175] to Y.M. from the Japan Society for the Promotion of Science.

Acknowledgments: We thank Louise Adam, ELS(D), from Edanz Group (www.edanzediting.com/ac) for editing a draft of this manuscript.

Conflicts of Interest: The authors declare no conflicts of interest.

Abbreviations

α-MEM	alpha minimum essential medium
BSA	bovine serum albumin
CFU-F	colony forming unit-fibroblast
DAPI	4′,6-diamidino-2-phenylindole
Dex	dexamethasone
FBS	fetal bovine serum
FITC	fluorescein isothiocyanate
GFP	green fluorescent protein
MSC	mesenchymal stem cell
PBS	phosphate-buffered saline

References

1. Uchiyama, A.; Motegi, S.; Sekiguchi, A.; Fujiwara, C.; Perera, B.; Ogino, S.; Yokoyama, Y.; Ishikawa, O. Mesenchymal stem cells-derived MFG-E8 accelerates diabetic cutaneous wound healing. *J. Dermatol. Sci.* **2017**, *86*, 187–197. [CrossRef]
2. Mouiseddine, M.; Mathieu, N.; Stefani, J.; Demarquay, C.; Bertho, J.M. Characterization and histological localization of multipotent mesenchymal stromal cells in the human postnatal thymus. *Stem Cells Dev.* **2008**, *17*, 1165–1174. [CrossRef]
3. Payne, N.L.; Sun, G.; Mcdonald, C.; Layton, D.; Moussa, L.; Emerson-Webber, A.; Veron, N.; Siatskas, C.; Herszfeld, D.; Price, J.; et al. Distinct immunomodulatory and migratory mechanisms underpin the therapeutic potential of human mesenchymal stem cells in autoimmune demyelination. *Cell Transplant.* **2013**, *22*, 1409–1425. [CrossRef]
4. Oh, S.Y.; Lee, S.J.; Jung, Y.; Lee, H.J.; Han, H.J. Arachidonic acid promotes skin wound healing through induction of human MSC migration by MT3-MMP-mediated fibronectin degradation. *Cell Death Dis.* **2015**, *6*, e1750. [CrossRef]
5. Huang, S.; Xu, L.; Zhang, Y.; Sun, Y.; Li, G. Systemic and Local Administration of Allogeneic Bone Marrow-Derived Mesenchymal Stem Cells Promotes Fracture Healing in Rats. *Cell Transplant.* **2015**, *24*, 2643–2655. [CrossRef]
6. Gupta, N.; Su, X.; Popov, B.; Lee, J.W.; Serikov, V.; Matthay, M.A. Intrapulmonary Delivery of Bone Marrow-Derived Mesenchymal Stem Cells Improves Survival and Attenuates Endotoxin-Induced Acute Lung Injury in Mice. *J. Immunol.* **2007**, *179*, 1855–1863. [CrossRef]
7. Ge, J.; Guo, L.; Wang, S.; Zhang, Y.; Cai, T.; Zhao, R.C.H.; Wu, Y. The Size of Mesenchymal Stem Cells is a Significant Cause of Vascular Obstructions and Stroke. *Stem Cell Rev. Rep.* **2014**, *10*, 295–303. [CrossRef]

8. Karp, J.M.; Leng, T.G. Mesenchymal Stem Cell Homing: The Devil Is in the Details. *Cell Stem Cell* **2009**, *4*, 206–216. [CrossRef] [PubMed]
9. Zhang, L.; Li, K.; Liu, X.; Li, D.; Luo, C.; Fu, B.; Cui, S.; Zhu, F.; Zhao, R.C.; Chen, X. Repeated Systemic Administration of Human Adipose-Derived Stem Cells Attenuates Overt Diabetic Nephropathy in Rats. *Stem Cells Dev.* **2013**, *22*, 3074–3086. [CrossRef] [PubMed]
10. Bazhanov, N.; Ylostalo, J.H.; Bartosh, T.J.; Tiblow, A.; Mohammadipoor, A.; Foskett, A.; Prockop, D.J. Intraperitoneally infused human mesenchymal stem cells form aggregates with mouse immune cells and attach to peritoneal organs. *Stem Cell Res. Ther.* **2016**, *7*, 27. [CrossRef] [PubMed]
11. Ezquer, M.; Urzua, C.A.; Montecino, S.; Leal, K.; Conget, P.; Ezquer, F. Intravitreal administration of multipotent mesenchymal stromal cells triggers a cytoprotective microenvironment in the retina of diabetic mice. *Stem Cell Res. Ther.* **2016**, *7*, 42. [CrossRef] [PubMed]
12. Himeoka, Y.; Kaneko, K. Enzyme oscillation can enhance the thermodynamic efficiency of cellular metabolism: Consequence of anti-phase coupling between reaction flux and affinity. *Phys. Biol.* **2016**, *13*, 026002. [CrossRef] [PubMed]
13. Aali, E.; Mirzamohammadi, S.; Ghaznavi, H.; Madjd, Z.; Larijani, B.; Rayegan, S.; Sharifi, A.M. A comparative study of mesenchymal stem cell transplantation with its paracrine effect on control of hyperglycemia in type 1 diabetic rats. *J. Diabetes Metab. Disord.* **2014**, *13*, 76. [CrossRef] [PubMed]
14. Li, C.; Li, G.; Liu, M.; Zhou, T.; Zhou, H. Paracrine effect of inflammatory cytokine-activated bone marrow mesenchymal stem cells and its role in osteoblast function. *J. Biosci. Bioeng.* **2016**, *121*, 213–219. [CrossRef]
15. Burk, J.; Berner, D.; Brehm, W.; Hillmann, A.; Horstmeier, C.; Josten, C.; Paebst, F.; Rossi, G.; Schubert, S.; Ahrberg, A.B. Long-Term Cell Tracking following Local Injection of Mesenchymal Stromal Cells in the Equine Model of Induced Tendon Disease. *Cell Transplant.* **2016**, *25*, 2199–2211. [CrossRef]
16. Liu, Y.S.; Ou, M.E.; Liu, H.; Gu, M.; Lv, L.W.; Fan, C.; Chen, T.; Zhao, X.-H.; Jin, C.Y.; Zhang, X.; et al. The effect of simvastatin on chemotactic capability of SDF-1α and the promotion of bone regeneration. *Biomaterials* **2014**, *35*, 4489–4498. [CrossRef]
17. Matsuura, Y.; Atsuta, I.; Ayukawa, Y.; Yamaza, T.; Kondo, R.; Takahashi, A.; Ueda, N.; Oshiro, W.; Tsukiyama, Y.; Koyano, K. Therapeutic interactions between mesenchymal stem cells for healing medication-related osteonecrosis of the jaw. *Stem Cell Res Ther.* **2016**, *7*, 119. [CrossRef]
18. Rasband, W.S. ImageJ, U.S. National Institutes of Health: Bethesda, MD, USA, 1997–2018. Available online: https://imagej.nih.gov/ij/ (accessed on 28 November 2018).
19. Duscher, D.; Rennert, R.C.; Januszyk, M.; Anghel, E.; Maan, Z.N.; Whittam, A.J.; Perez, M.G.; Kosaraju, R.; Hu, M.S.; Walmsley, G.G.; et al. Aging disrupts cell subpopulation dynamics and diminishes the function of mesenchymal stem cells. *Sci. Rep.* **2014**, *4*, 7144. [CrossRef]
20. Kurata, K.; Heino, T.J.; Higaki, H.; Väänänen, H.K. Bone marrow cell differentiation induced by mechanically damaged osteocytes in 3D gel-embedded culture. *J. Bone Miner. Res.* **2006**, *21*, 616–625. [CrossRef]
21. Atsuta, I.; Yamaza, T.; Yoshinari, M.; Goto, T.; Kido, M.A.; Kagiya, T.; Mino, S.; Shimono, M.; Tanaka, M. Ultrastructural localization of laminin-5 (γ2 chain) in the rat peri-implant oral mucosa around a titanium-dental implant by immuno-electron microscopy. *Biomaterials* **2005**, *26*, 6280–6287. [CrossRef]
22. Atsuta, I.; Yamaza, T.; Yoshinari, M.; Mino, S.; Goto, T.; Kido, M.A.; Terada, Y.; Tanaka, T. Changes in the distribution of laminin-5 during peri-implant epithelium formation after immediate titanium implantation in rats. *Biomaterials* **2005**, *26*, 1751–1760. [CrossRef] [PubMed]
23. Takamori, Y.; Atsuta, I.; Nakamura, H.; Sawase, T.; Koyan, K.; Hara, Y. Histopathological comparison of the onset of peri-implantitis and periodontitis in rats. *Clin. Oral Implants Res.* **2017**, *28*, 163–170. [CrossRef] [PubMed]
24. Von, D.F.; Kramer, M.; Wermke, M.; Wehner, R.; Röllig, C.; Alakel, N.; Stölzel, F.; Parmentier, S.; Sockel, K.; Krech, M.; et al. Mesenchymal Stromal Cells for Treatment of Acute Steroid-Refractory Graft Versus Host Disease: Clinical Responses and Long-Term Outcome. *Stem Cells* **2016**, *34*, 357–366.
25. Li, X.H.; Gao, C.J.; Da, W.M.; Cao, Y.B.; Wang, Z.H.; Xu, L.X.; Wu, Y.M.; Liu, B.; Liu, Z.Y.; Yan, B.; et al. Reduced Intensity Conditioning, Combined Transplantation of Haploidentical Hematopoietic Stem Cells and Mesenchymal Stem Cells in Patients with Severe Aplastic Anemia. *PLoS ONE* **2014**, *9*, e89666. [CrossRef] [PubMed]
26. Antonio, U.; Lorenzo, M.; Vito, P. Mesenchymal stem cells in health and disease. *Nat. Rev. Immunol.* **2008**, *8*, 726–736.

27. Kondo, R.; Atsuta, I.; Ayukawa, Y.; Yamaza, T.; Matsuura, Y.; Furuhashi, A.; Tsukiyama, Y.; Koyano, K. Therapeutic interaction of systemically-administered mesenchymal stem cells with peri-implant mucosa. *PLoS ONE* **2014**, *9*, e90681. [CrossRef]
28. Kanazawa, M.; Atsuta, I.; Ayukawa, Y.; Yamaza, T.; Kondo, R.; Matsuura, Y.; Koyano, K. The influence of systemically or locally administered mesenchymal stem cells on tissue repair in a rat oral implantation model. *Int. J. Implant Dent.* **2018**, *4*, 2. [CrossRef]
29. Holder, A.J.; Badiei, N.; Hawkins, K.; Wright, C.; Williams, P.R.; Curtis, D.J. Control of collagen gel mechanical properties through manipulation of gelation conditions near the sol-gel transition. *Soft Matter* **2018**, *14*, 574–580. [CrossRef]
30. Kimura, H.; Ouchi, T.; Shibata, S.; Amemiya, T. Stem cells purified from human induced pluripotent stem cell-derived neural crest-like cells promote peripheral nerve regeneration. *Sci. Rep.* **2018**, *8*, 10071. [CrossRef]
31. Ogawa, M.; Ogawa, S.; Bear, C.E.; Ahmadi, S.; Chin, S.; Li, B. Directed differentiation of cholangiocytes from human pluripotent stem cells. *Nat. Biotechnol.* **2015**, *33*, 853–861. [CrossRef]
32. Xie, L.; Zhang, N.; Marsano, A.; Vunjak, N.G.; Zhang, Y.; Lopez, M.J. In vitro mesenchymal trilineage differentiation and extracellular matrix production by adipose and bone marrow derived adult equine multipotent stromal cells on a collagen scaffold. *Stem Cell Rev. Rep.* **2013**, *9*, 858–872. [CrossRef] [PubMed]
33. Hou, C.; Shen, L.; Huang, Q.; Mi, J.; Wu, Y.; Yang, M.; Zeng, W.; Li, L.; Chen, W.; Zhu, C. The effect of heme oxygenase-1 complexed with collagen on MSC performance in the treatment of diabetic ischemic ulcer. *Biomaterials* **2013**, *34*, 112–120. [CrossRef] [PubMed]
34. Nakagawa, H.; Isaji, M.; Hayashi, M.; Tsurufuji, S. Selective inhibition of collagen breakdown by proteinase inhibitors in granulation tissue in rats. *J. Biochem.* **1981**, *89*, 1081–1090. [PubMed]
35. Kühl, T.; Mezger, M.; Hausser, I.; Handgretinger, R.; Bruckner, T.L.; Nyström, A. High local concentrations of intradermal MSCs restore skin integrity and facilitate wound healing in dystrophic epidermolysis bullosa. *Mol. Ther.* **2015**, *23*, 1368–1379. [CrossRef]
36. Lee, R.H.; Pulin, A.A.; Seo, M.J.; Kota, D.J.; Ylostalo, J.; Larson, B.L.; Semprun-Prieto, L.; Delafontaine, P.; Prockop, D.J. Intravenous hMSCs improve myocardial infarction in mice because cells embolized in lung are activated to secrete the anti-inflammatory protein TSG-6. *Cell Stem Cell* **2009**, *5*, 54–63. [CrossRef]
37. Nagaishi, K.; Ataka, K.; Echizen, E.; Arimura, Y.; Fujimiya, M. Mesenchymal stem cell therapy ameliorates diabetic hepatocyte damage in mice by inhibiting infiltration of bone marrow-derived cells. *Hepatology* **2014**, *59*, 1816–1829. [CrossRef]
38. Zhang, Q.; Nguyen, P.; Xu, Q.; Park, W.; Lee, S.; Furuhashi, A. Neural Progenitor-Like Cells Induced from Human Gingiva-Derived Mesenchymal Stem Cells Regulate Myelination of Schwann Cells in Rat Sciatic Nerve Regeneration. *Stem Cells Transl Med* **2016**, *5*, 1–13. [CrossRef]
39. Peired, A.J.; Sisti, A.; Romagnani, P. Mesenchymal Stem Cell-based therapy for kidney disease: A Review of clinical evidence. *Stem Cells Int.* **2016**, 4798639. [CrossRef]
40. Elizabeth, B.; Yanzhou, L.; Li, C.; Austin, M.G. Eicosanoids: Emerging contributors in stem cell-mediated wound Healing. *Prostaglandins Other Lipid Mediat.* **2016**, *132*, 17–24.
41. Yu, Y.; Wu, R.X.; Gao, L.N.; Xia, Y.; Tang, H.N.; Chen, F.M. Stromal cell-derived factor-1-directed bone marrow mesenchymal stem cell migration in response to inflammatory and/or hypoxic stimuli. *Cell Adh. Migr.* **2016**, *10*, 342–359. [CrossRef]